# CHAPTER IV

# RESULTS AND DISCUSSION

## 4.1 Preliminary study on the degradation of PET surface by UV irradiation

The PET sample was primarily studied by irradiating UV light through the diamond μATR probe. The diamond has an optical contact with the PET surface. The degraded PET surface was initially investigated by FT-IR microscope spectrometer. Since the diamond μATR probe is a homemade construction, it is necessary to compare ATR spectra acquired by the μATR probe and that acquired by the conventional ATR. The observed ATR spectra of PET by both techniques were shown in Fig. 4.1.

Both diamond μATR and conventional ATR accessories gave the same spectra. The observed spectra showed main absorption band associated with the chemical composition and structure of PET. The PET spectrum contained main bands associated with ester, aromatic and aliphatic hydrocarbon moieties. The band assignments of PET were shown in Table 4.1.

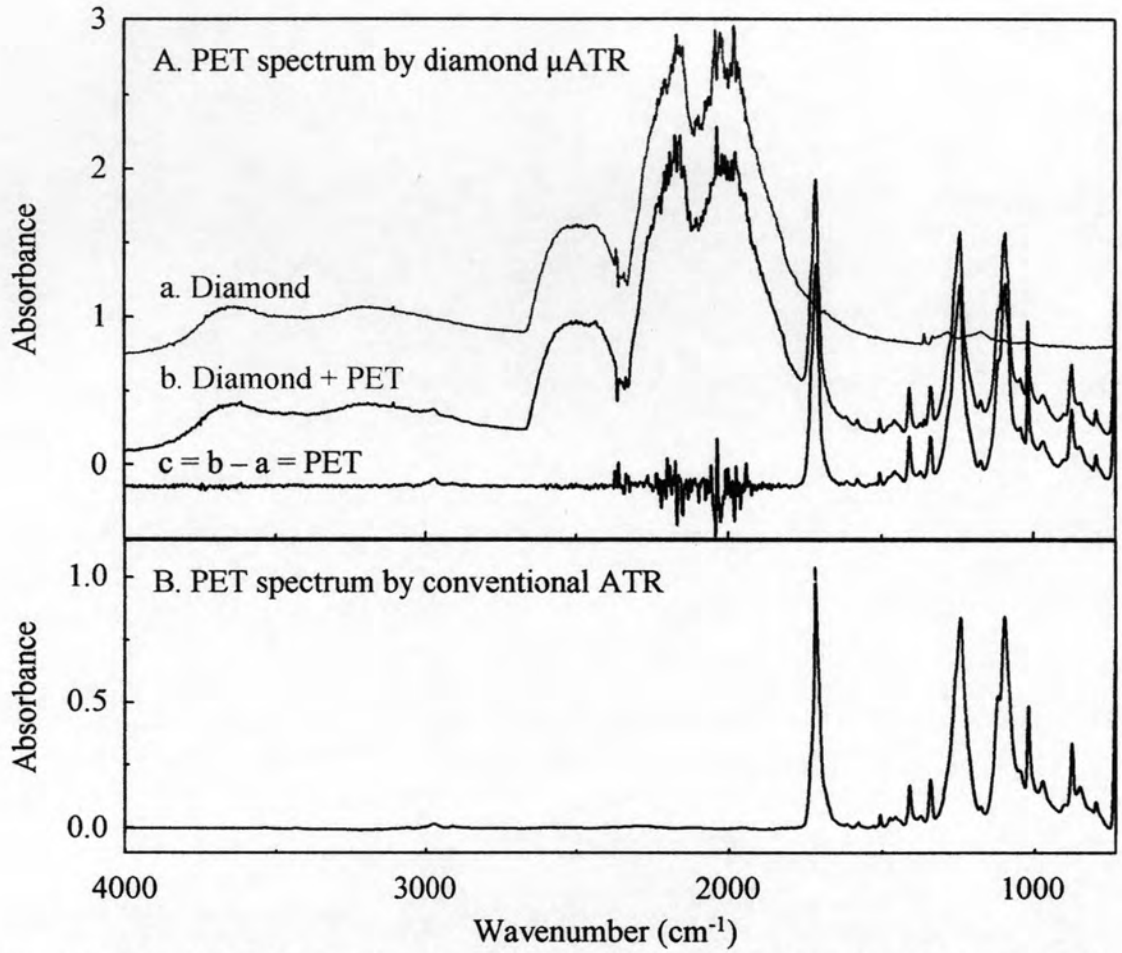


Fig. 4.1 The ATR FT-IR spectra of an un-irradiated PET acquired by using the homemade diamond μATR and the conventional ATR with a 45° ZnSe IRE: (A) The observed PET spectra by diamond μATR; (a) Transflectance spectra of diamond, (b) ATR spectra of PET and transflectance spectra of diamond, and (c) Diamond-ATR spectra of PET and (B) The observed PET spectrum by conventional ATR.

Table 4.1 Infrared band assignments of un-irradiated PET

| Wavenumber ($cm^{-1}$) | Bands assignment |
|---|---|
| 3440 | O-H stretching of ethylene glycol end-groups |
| 3076 | Aromatic C-H stretching |
| 2973, 2908 | Aliphatic C-H stretching |
| 1715 | C=O stretching of aromatic ester |
| 1371, 1338 | $-CH_2-$ wagging |
| 1239, 1097 | Asymmetric and symmetric stretching of C-O-C group of aromatic ester |
| 1613 | C=C stretching vibration of aromatic ring |
| 1578, 1505, 1408 | Skeletal vibration of aromatic ring conjugation |
| 1173, 1117, 1017 | Skeletal ring indicated 1,4-substitution |
| 871 | C-H deformation of aromatic ring |

Before the PET film was irradiated under the UV-ATR condition, the contact between PET sample and diamond IRE was optimized in order to ensure that the changes were caused by the irradiation. The PET film was placed at the culet of diamond IRE while an external force was applied onto the specimen against the IRE. All ATR FT-IR spectra were subsequently collected after the pressure was increased. Spectra were collected until the spectral intensity was unchanged as shown in Fig. 4.2. After the constant spectra of PET were observed PET spectra, the UV radiation was coupled to homemade diamond μATR probe for 1, 10 and 30 minutes, respectively. ATR spectra of irradiated film were acquired by FT-IR microscope spectrometer.

ATR FT-IR spectra of irradiated PET under the UV evanescent field irradiation were compared with that of photo-degradation generated by the conventional UV transmission and un-irradiated PET as shown in Fig. 4.3.

The irradiated PET samples under the UV evanescent field at various irradiation times were compared with that of the un-irradiated PET. The changes were varied with the irradiation times. The changes caused by UV evanescent field irradiation and UV transmission were similar. The irradiated PET spectra revealed the

change of carbonyl region (1600-1800 $cm^{-1}$) and showed broader band at hydroxyl region (2750-3650 $cm^{-1}$). The hydroxyl region became broader which indicated the -OH stretching of alcohol and carboxylic. At the carbonyl region, the spectra observed a band broadening and decreasing peak height of ester. This change indicated new carbonyl species (i.e., carboxylic acid or aldehyde) that were formed [6, 31, 35]. These results supported the UV evanescent field induced degradation of PET. These changes indicated new species associated to the chemical changes on the PET surface due to photo-degradation. The increment of hydroxyl and carboxylic groups might be followed photo-oxidation reaction and Norrish type I, II reactions [6, 28].

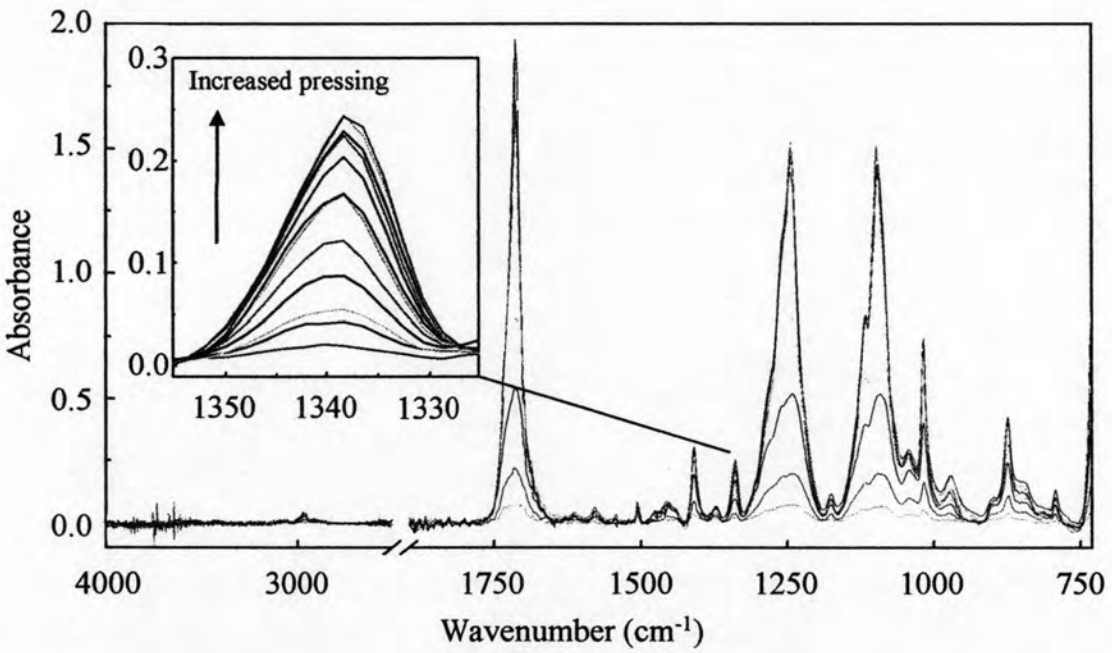


Fig. 4.2 ATR FT-IR spectra of PET after a subsequent increment of pressure.

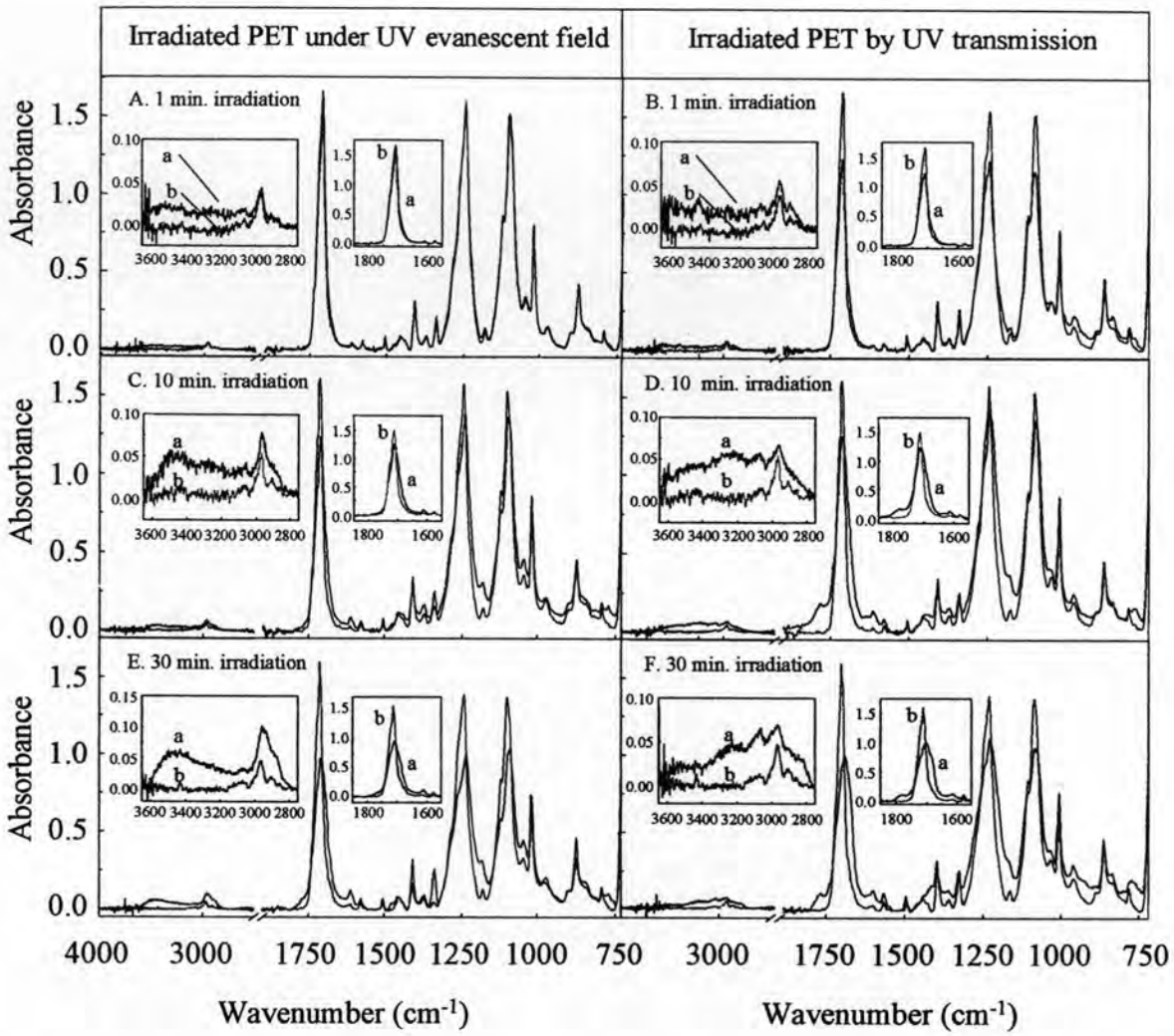


Fig. 4.3 ATR FT-IR spectra of irradiated PET at various irradiation times: (A), (C) and (E) at 1, 10, 30 minutes under the UV evanescent field and (B), (D) and (F) at 1, 10, 30 minutes by UV transmission: (a) irradiated PET and (b) un-irradiated PET.

The spectra of irradiated PET under the UV evanescent field irradiation supported the novel technique for improving hydrophilicity of PET. Although UV evanescent field irradiation can be induced the surface degradation of PET, at long irradiation time (such as 30 minutes) was not suitable for application in industries because the industrial processes needed a high speed throughput operation. Thus, this research was focused on short irradiation times (1-10 minutes) in the further study and application for various PET types available in industries.

## 4.2 Degradation of PET by UV irradiations

### 4.2.1 Degradation by the UV transmission irradiation

PET samples were irradiated by conventional UV transmission at 1-10 min. The infrared spectra of the irradiated samples were collected by conventional ATR and diamond μATR, as shown in Fig. 4.4-4.5, respectively.

The irradiated PET spectra were compared with that of un-irradiated PET. According to the observed spectra, the spectral results indicated that the changes of physical and chemical properties. The external PET texture which is transparent was changed into yellow-orange at the exposed side and white color on the opposite side. The observed color change was increased as the irradiation time was increased. This color was easily observed and was a good indicator for the physical properties changing in the bulk. The color formations occur due to photo-degradation and chain transformation. The photo-degradation process under ambient condition can induce the photo-oxidation reaction that produced the dihydroxyl compound. This hydroxyl compound is a chromophore group which occurs continuously and produces colored species (quinone compound) [6, 37]. In addition, the changes of transparent sample to white color or opaque sample are involved the phase transformation from amorphous to crystalline that caused a change of mechanical properties. The irradiated PET spectra of both diamond μATR and conventional ATR revealed the same change of chemical properties as discussed in preliminary study section. The observed spectra change of irradiated PET at various times showed step-by-step chemical changes which were irradiated by UV transmission as shown in Table 4.2.

The spectral changes of irradiated PET by UV transmission at various irradiation times were plotted against the irradiation times. The peak area of the hydroxyl region at 2750-3650 $cm^{-1}$ (O-H stretching and –CH stretching) was compared with the aromatic skeletal at 1505 $cm^{-1}$. The constant peak of aromatic skeletal without normalization process (unchanged peak under the UV irradiation) was employed as an internal standard. Both hydroxyl region and aromatic skeletal were plotted against the irradiation times as shown in Fig. 4.6. The exact peak area was shown in Table 4.3.

The hydroxyl region showed increment of the area as the irradiated times were increased and became constant after 5 minutes. Thus, the higher irradiation time may not improve the hydroxyl group.

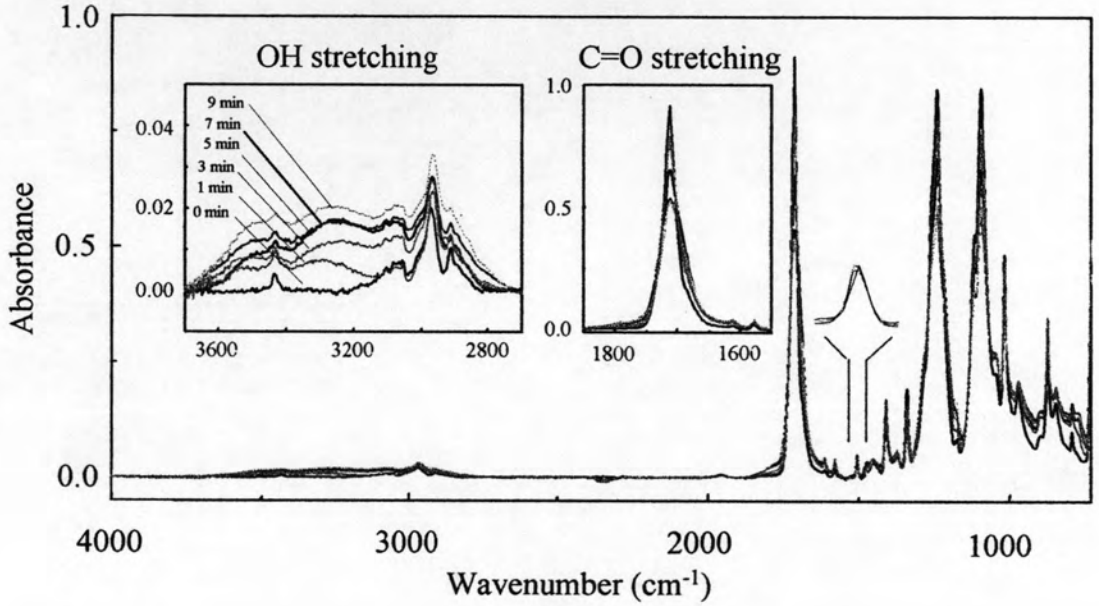


Fig. 4.4 Conventional ATR FT-IR spectra of irradiated PET by UV transmission.

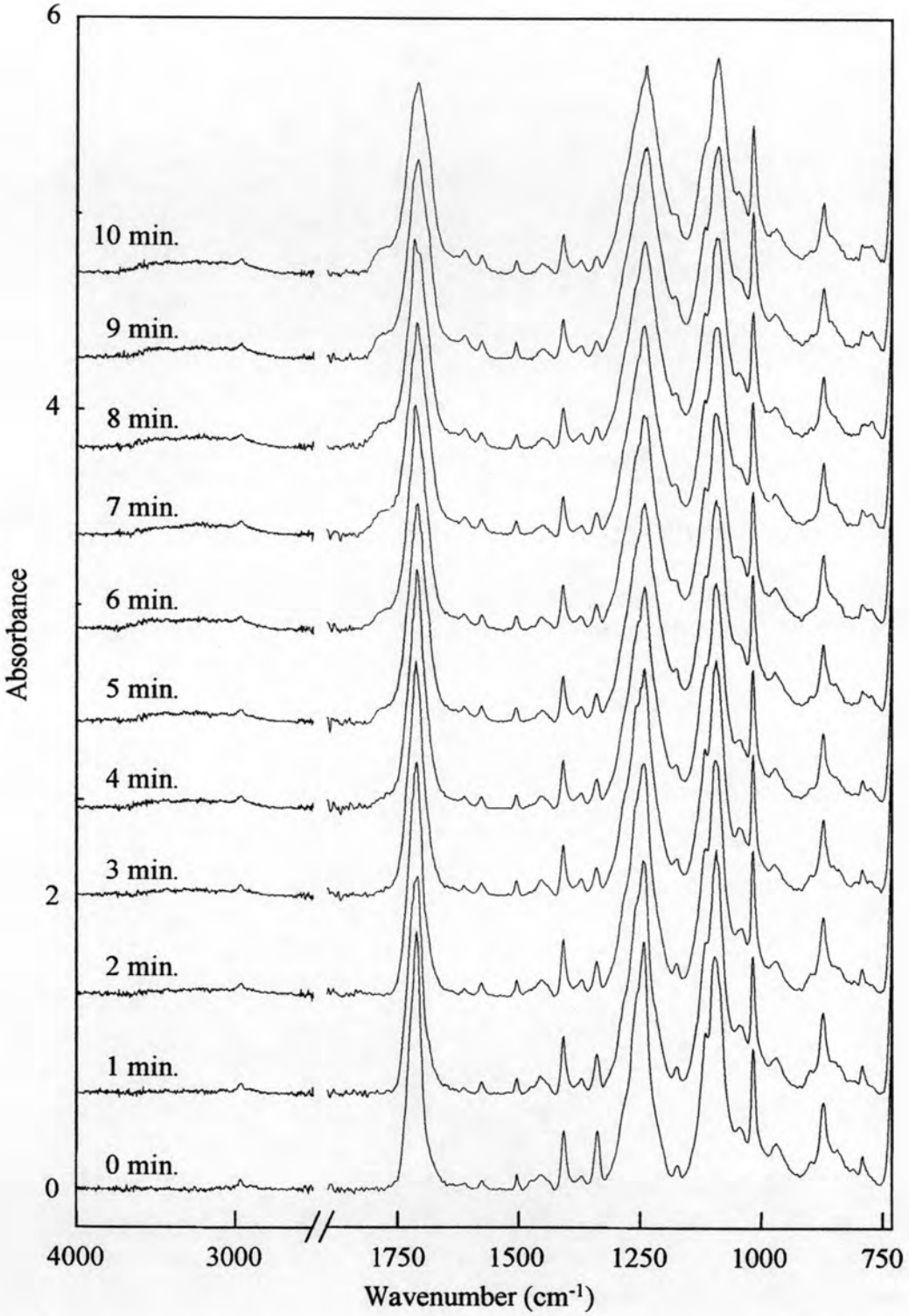


Fig. 4.5 Diamond μATR FT-IR spectra of PET after the irradiation under UV transmission for 1-10 minutes.

Table 4.2 The observed spectra changes of irradiated PET by UV transmission

| Wavenumber ($cm^{-1}$) | Observed spectra changes | Associated chemical information |
|---|---|---|
| 3650-2750 | New peak and band broadening | New hydroxyl species generated at the surface. |
| 1715 | Decreasing peak height and band broadening | Some of the ester carbonyl changed to new carbonyl species (i.e., acid carbonyl). |
| 1239, 1097 | Decreasing peak height and band broadening | The C-O of ester changed to carbonyl species. |
| 1371 | Increasing peak height | The peak is indicated as gauche conformer of amorphous phase in PET. |
| 1338 | Decreasing peak height | The peak is indicated as *trans* conformer of crystalline phase in PET. |

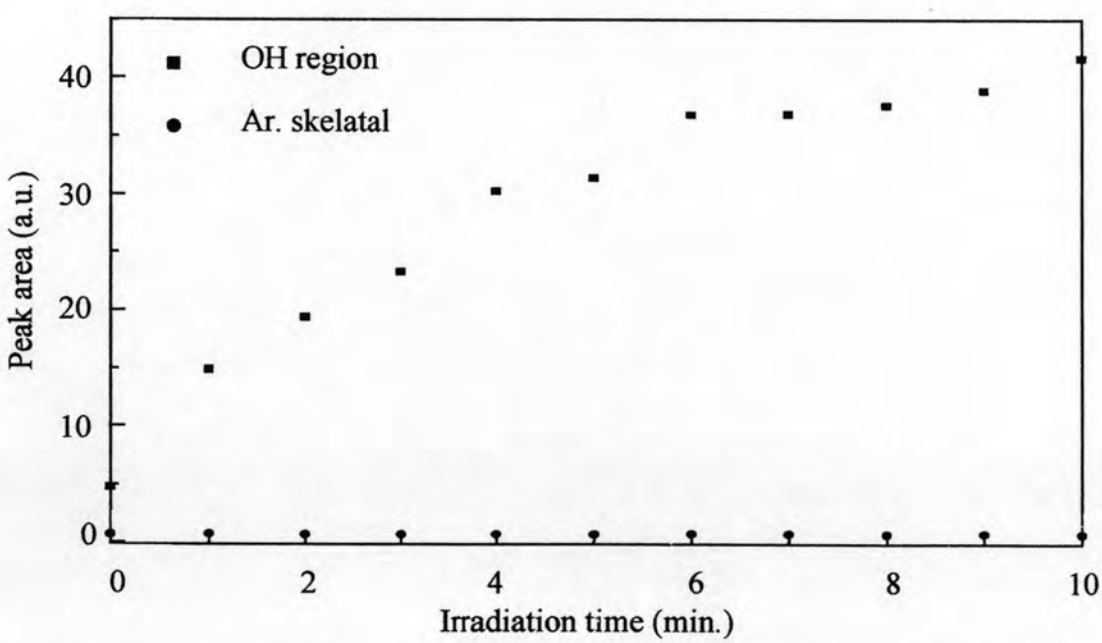


Fig. 4.6 Area plot of hydroxyl region at 2750-3650 $cm^{-1}$ (-OH stretching and –CH stretching) and aromatic skeletal at 1505 $cm^{-1}$ at various irradiation times.

Table 4.3 Area of hydroxyl region and aromatic skeletal of irradiated PET by UV transmission at various irradiation.

| Irradiation time (min.) | Peak area (a.u.) | |
|---|---|---|
| | Hydroxyl region at 2750-3650 $cm^{-1}$ | C=C aromatic skeletal at 1505 $cm^{-1}$ |
| 0 | 4.705 | 0.641 |
| 1 | 14.836 | 0.675 |
| 2 | 19.349 | 0.621 |
| 3 | 23.287 | 0.640 |
| 4 | 30.251 | 0.668 |
| 5 | 31.385 | 0.641 |
| 6 | 36.798 | 0.687 |
| 7 | 36.845 | 0.688 |
| 8 | 37.593 | 0.655 |
| 9 | 38.853 | 0.684 |
| 10 | 41.664 | 0.657 |

### 4.2.2 Degradation by the UV evanescent field irradiation

The PET samples were irradiated under the UV evanescent field and collected infrared spectra by using diamond μATR. The external character of irradiated PET film at 1-10 minutes showed an un-noticeable change on the surface. However, the ATR FT-IR spectra revealed the chemical changes with increasing irradiation time as shown in Fig. 4.7.

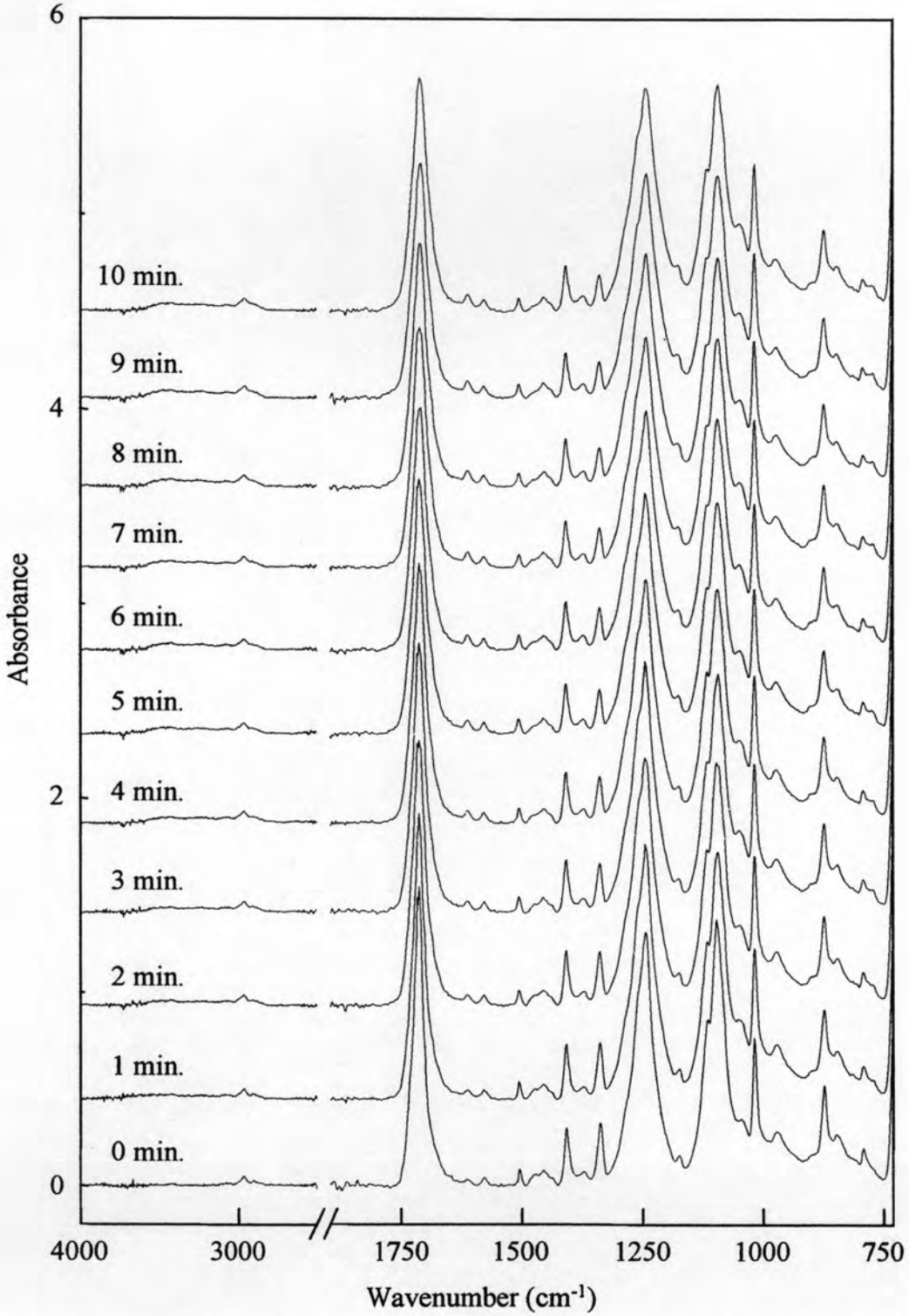


Fig. 4.7 Diamond μATR FT-IR spectra of PET film after the UV evanescent field for 1-10 minutes.

The changing spectral feature of the irradiated PET film under the UV evanescent field was observed. Plots of hydroxyl region (O-H stretching and –CH stretching at 2750-3650 $cm^{-1}$) and aromatic skeletal area (C=C at 1505 $cm^{-1}$) against the irradiation times were shown in Fig. 4.8. The corresponding exact values were shown in Table 4.4.

The absorption in the hydroxyl region was increased as the irradiation times were increased and became constant after 5 minutes irradiation. According to the spectra changes, this irradiation times may be optimized for improving hydrophilicity because the hydrophilic property depends on the amount of hydroxyl group.

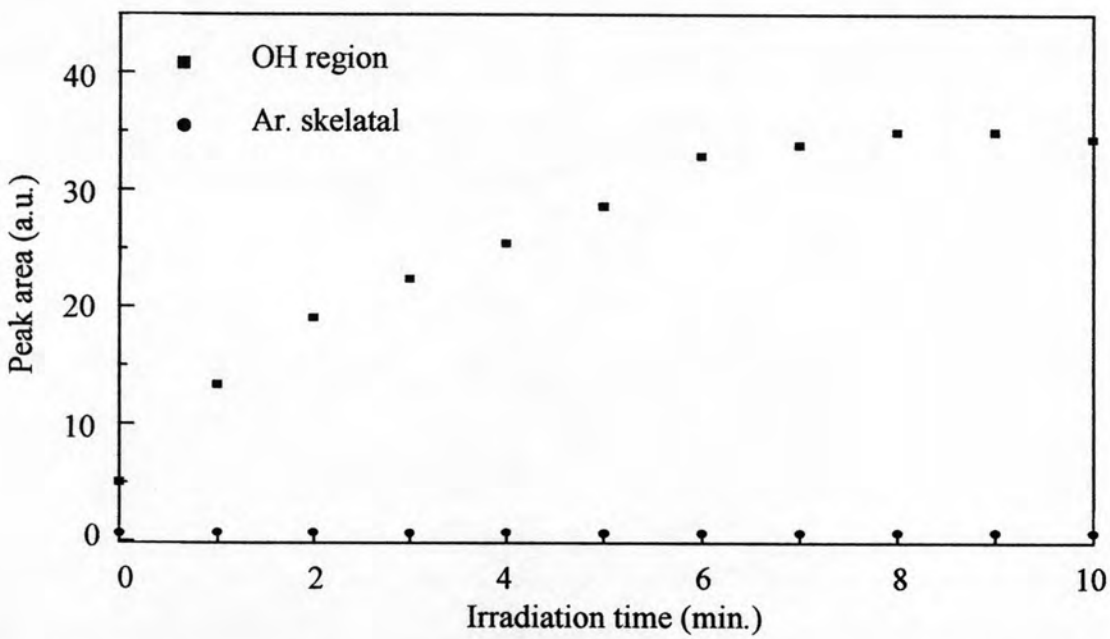


Fig. 4.8 Area plotting of hydroxyl region at 2750-3650 $cm^{-1}$ (-OH stretching and –CH stretching) and aromatic skeletal at 1505 $cm^{-1}$ at various irradiation times.

Table 4.4 Area of hydroxyl region and C=C aromatic skeletal of irradiated PET under UV evanescent field at various irradiation times.

| Irradiation time (min.) | Peak area (a.u.) | |
|---|---|---|
| | Hydroxyl region at 2750-3650 $cm^{-1}$ | C=C aromatic skeletal at 1505 $cm^{-1}$ |
| 0 | 4.982 | 0.657 |
| 1 | 13.329 | 0.696 |
| 2 | 19.054 | 0.721 |
| 3 | 22.363 | 0.646 |
| 4 | 25.430 | 0.718 |
| 5 | 28.586 | 0.636 |
| 6 | 32.884 | 0.621 |
| 7 | 33.823 | 0.648 |
| 8 | 34.923 | 0.673 |
| 9 | 34.943 | 0.674 |
| 10 | 34.345 | 0.648 |

## 4.3 Comparison of irradiated PET by both the UV evanescent field and UV transmission irradiations

### 4.3.1 Curve fitting ATR FT-IR spectra

The irradiated PET samples by UV transmission and evanescent field irradiation at 10 minutes were compared with that of the un-irradiated PET film, as shown in Fig. 4.9.

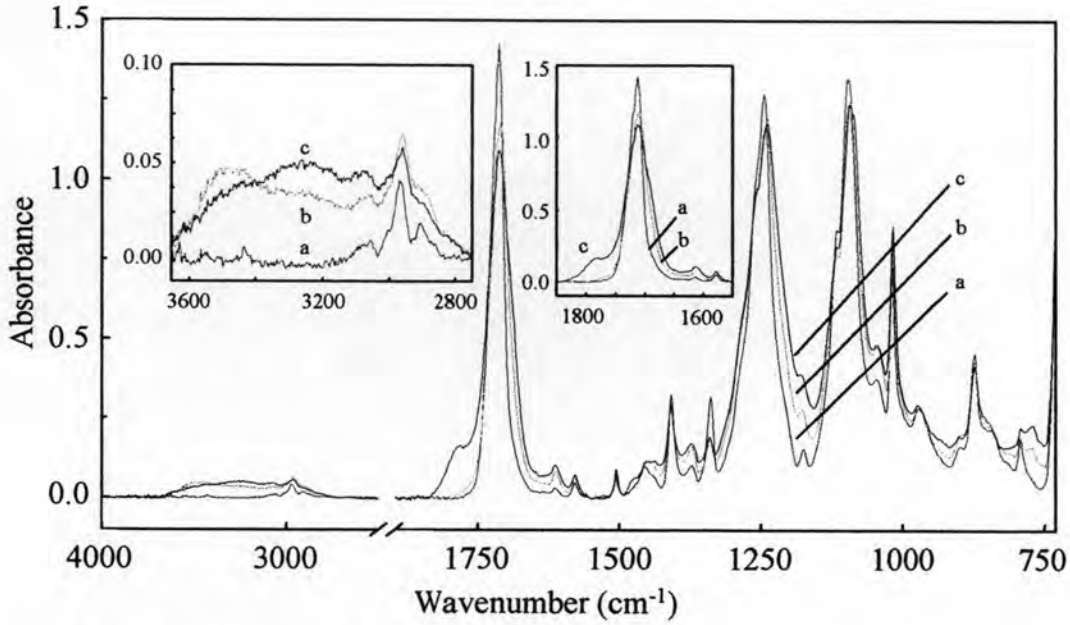


Fig. 4.9 The ATR FT-IR spectra of irradiated PET by both techniques and un-irradiated PET: (a) spectrum of un-irradiated PET, (b) spectrum of PET under the UV evanescent field irradiation, and (c) spectrum of PET by UV transmission.

Although, the observed spectra changes of irradiated PET by both UV techniques showed similar change, these spectral results indicated a greater degree of degradation by UV transmission compared to that of the UV evanescent field irradiation. The band broadening of the hydroxyl and carbonyl regions of irradiated PET by UV transmission were greater than those of UV evanescent field irradiation. Since UV evanescent field has a penetration depth of approximately 90 nm from the surface (365 nm, 45 degrees with diamond IRE), the bulk properties were expected to be unchanged. This discussion was verified by the collected ATR FT-IR spectra of the exposed side and the opposite side in comparison with that of un-irradiated PET. The irradiated PET spectra of exposed side by UV transmission were compared with that of opposite side and un-irradiated PET, as shown in Fig. 4.10.

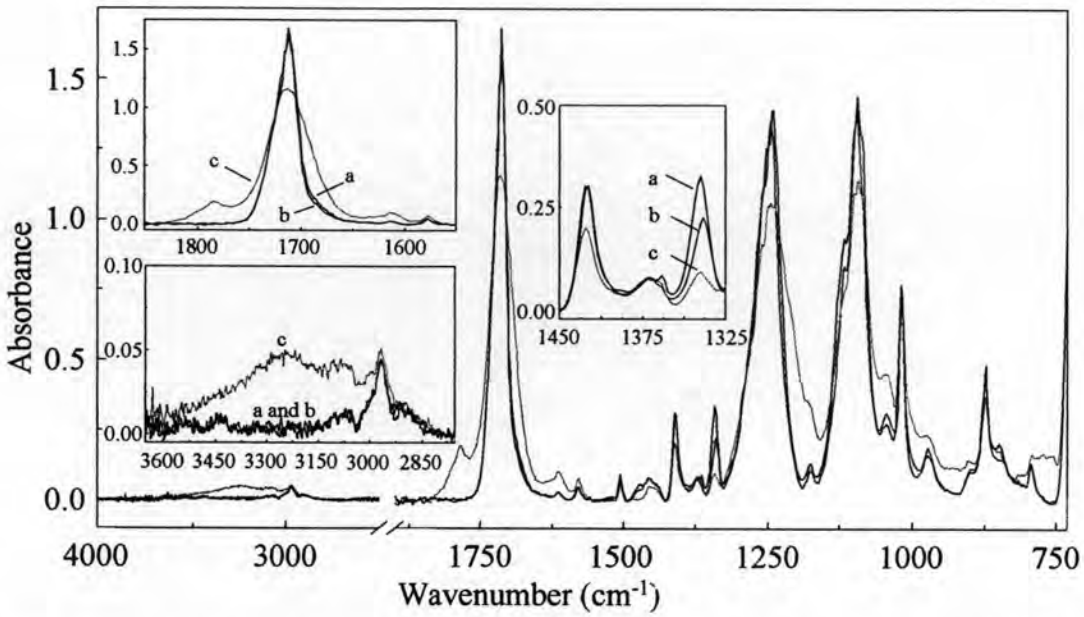


Fig. 4.10 ATR spectra of the exposed side and the opposite side of the PET film after the UV transmission irradiation were compared with that of the un-irradiated PET: (a) opposite side of irradiated PET, (b) un-irradiated PET, and (c) exposed side of irradiated PET.

From this result, both the infrared spectra of the opposite side and the exposed side of irradiated PET by UV transmission were compared with that of un-irradiated PET. Since the collected ATR spectra conditions of all samples may not be exactly the same, the absorption at 1505 $cm^{-1}$ of aromatic ring skeletal, which was unchanged by any irradiation condition, was employed as an indicator for the same sampling condition. All compared spectra must have the same absorption at 1505 $cm^{-1}$. The spectrum of exposed side obviously showed different chemical characteristic from ATR spectra of opposite side and un-irradiated PET due to photo-degradation. The spectrum of opposite side of the irradiated PET did not show any sign of degradation. However, the spectrum of opposite side was not the same as that of the un-irradiated PET. It showed significant changes at 1338 $cm^{-1}$ and 1371 $cm^{-1}$. The band at 1338 $cm^{-1}$ indicated the *trans* conformation of ethylene glycol group orientation associated with crystallinity in PET structure. On the other hand, the band at 1371 $cm^{-1}$ indicated the *gauche* conformation of ethylene glycol segment that related to amorphous phase in PET [12, 38-40].

The band width at 1338 $cm^{-1}$ of the opposite side of the irradiated PET was grater than that of the un-irradiated PET and less than that of the irradiated PET at 1371 $cm^{-1}$. It indicated that there was increasing the crystalline phase in the bulk and amorphous phase at the surface of irradiated PET by the UV transmission irradiation. The crystallinity of the PET film was increasing by conformation change from the *gauche* conformation to the *trans* conformation. The *trans* conformation can be increased by various methods such as annealing process [41]. In the case of irradiated PET by UV radiation, the PET samples can absorb the UV radiation and emit the thermal energy. A thermocouple can detect the high temperature (approximately temperature 170 ℃) at the PET surface during UV transmission due to heat emission, which was higher than glass transition temperature of PET ($T_g \approx 67$ ℃ ), but it was less than melting temperature ($T_m \approx 250$ ℃ ) and degradation temperature ($T_d \approx 345$ ℃ [41]). Therefore, the conformation changes occur by the annealing process. The annealing process which occurred at high temperature during secondary crystallization can be formed new single crystals from the amorphous phase [42]. An infrared spectrum of annealed PET at 170 ℃ was compared with that of un-irradiated PET, as shown in Fig. 4.11.

Fig. 4.11 showed the same spectral changes observed at the opposite side of the irradiated PET by UV transmission. This confirms the annealing process of the opposite side that causing the change in the bulk properties of irradiated PET was due to the UV irradiation.

In the case of irradiated PET under the UV evanescent field, the spectra of the exposed side and the opposite side were compared with that of un-irradiated PET, as shown in Fig. 4.12.

The observed spectra at 1338 $cm^{-1}$ and 1371 $cm^{-1}$ of the exposed side were the same as the exposed side of irradiated PET by UV transmission. When the un-irradiated PET spectrum was compared with that of opposite side of irradiated PET under the UV evanescent field irradiation, the observed spectral changes of the opposite side were not detected. Since the UV evanescent field was only penetrated to the PET surface, the bulk properties of PET were expected to be unchanged.

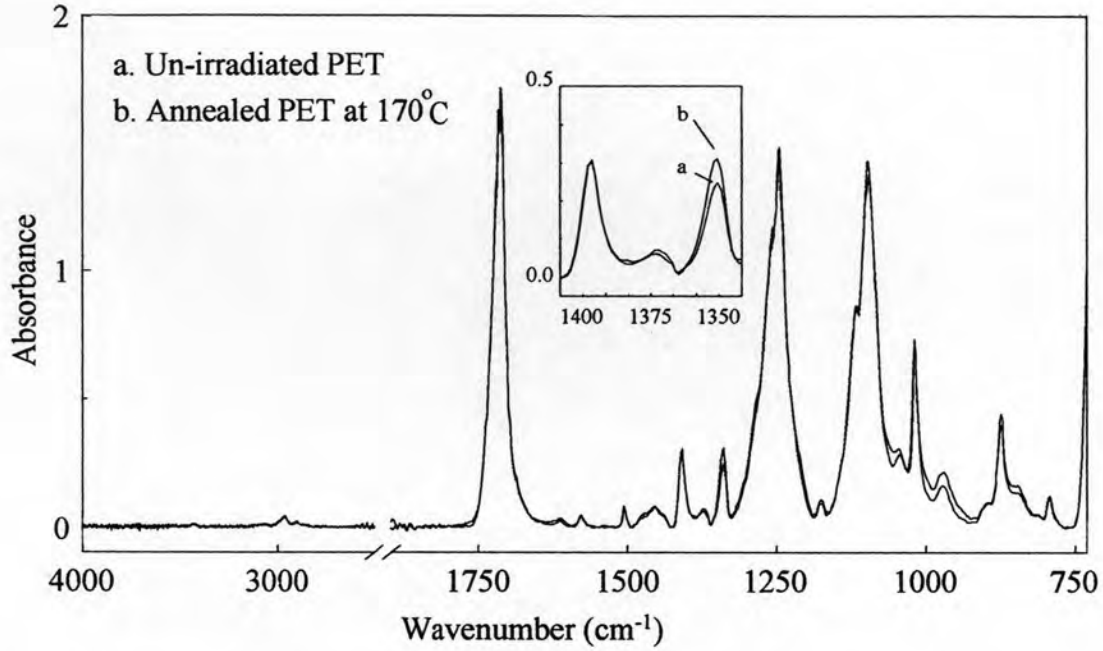


Fig. 4.11 The un-irradiated PET spectrum compared with that of annealed PET: (a) un-irradiated PET and (b) annealed PET at 170℃ for 10 minutes.

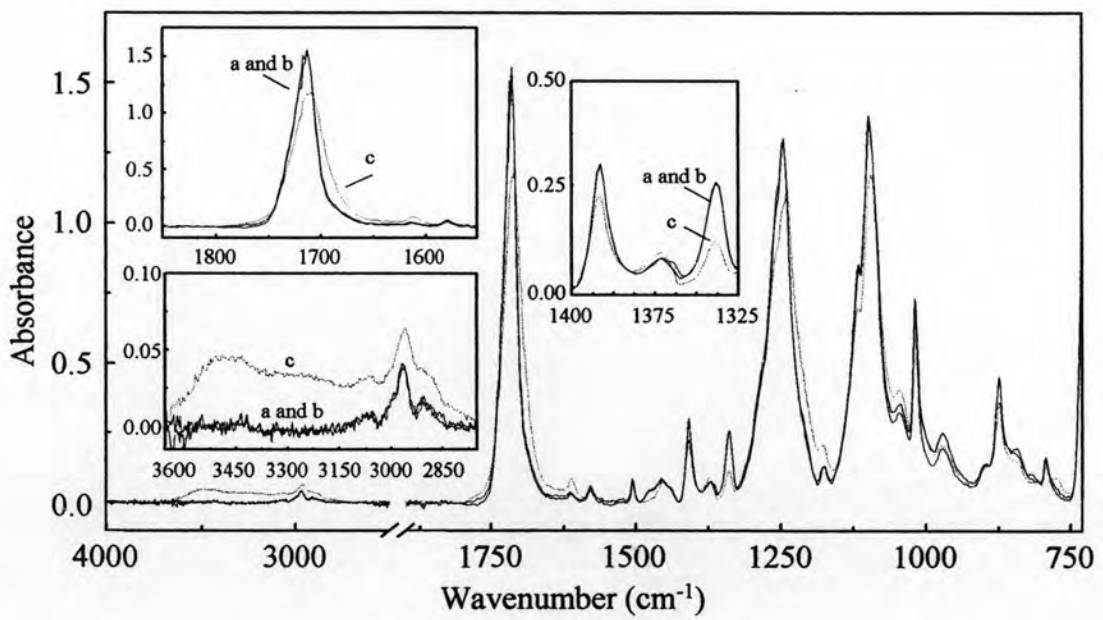


Fig. 4.12 The ATR spectra of irradiated PET both the exposed side and the opposite side under the UV evanescent field irradiation were compared with that of un-irradiated PET: (a) the opposite side of irradiated PET, (b) the un-irradiated PET, and (c) the exposed side of irradiated PET.

Since the observed spectral changes of the irradiated PET under the UV evanescent field and the UV transmission were similar, curve fitting was employed for the identification of chemical species. The curve fitting can indicate different compositions of these bands. The hydroxyl region (2750-3650 $cm^{-1}$) of irradiated PET at 10 minutes irradiation was analyzed. Seven bands were revealed and shown in Fig. 4.13.

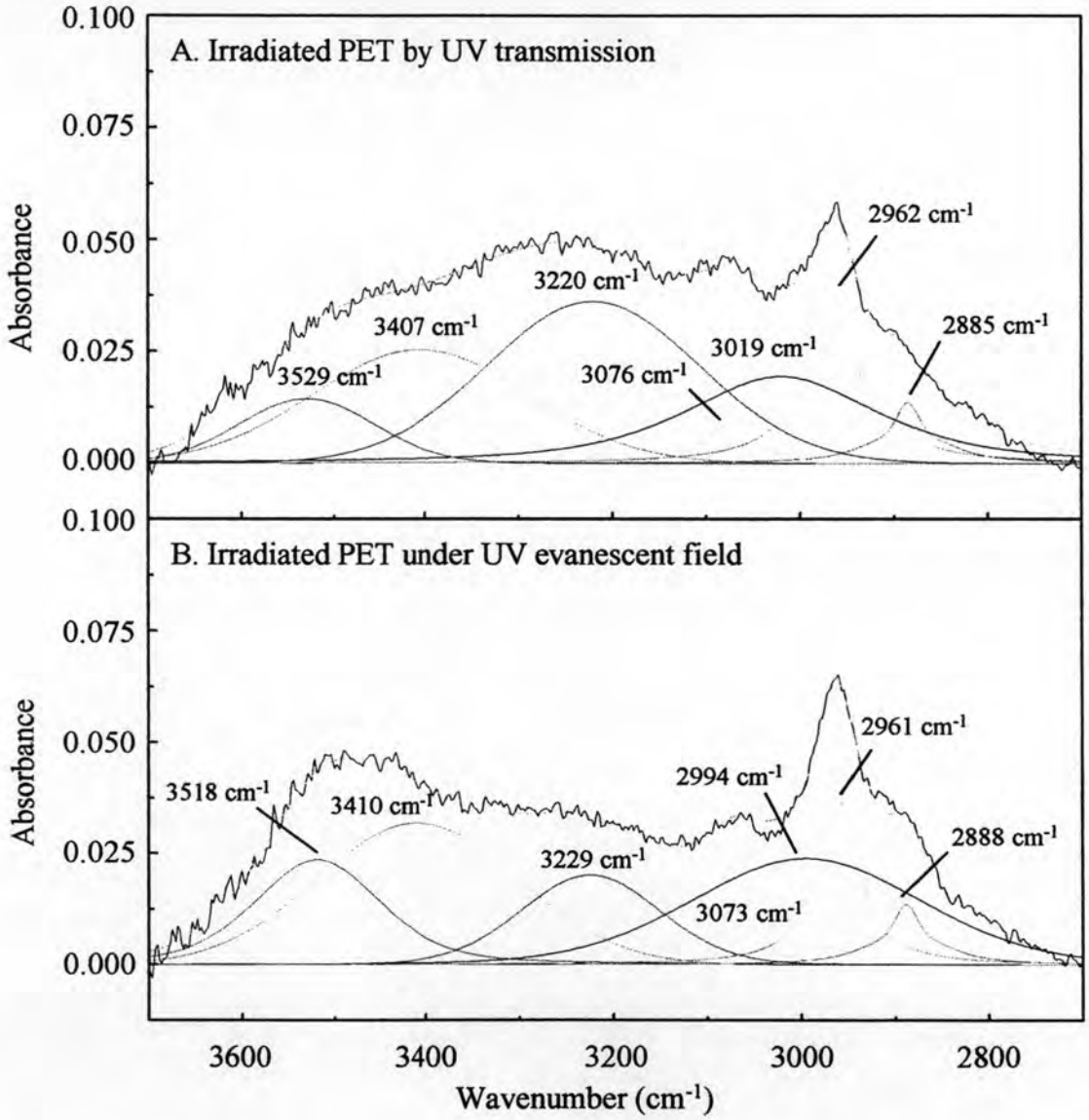


Fig. 4.13 Curve fitting of hydroxyl region in both irradiation techniques: (A) irradiated PET by UV transmission and (B) irradiated PET under UV evanescent field.

The hydroxyl region of irradiated PET by both irradiations consist the bands of hydroxyl species, aromatic and aliphatic hydrocarbon. The C-H stretching of aliphatic hydrocarbon was approximately at 2885 $cm^{-1}$ and 2960 $cm^{-1}$. Aromatic hydrocarbon was approximately at 3075 $cm^{-1}$. The hydroxyl species show four peaks of O-H stretching at the surface indicating various hydrogen bond in the hydroxyl region of irradiated PET spectra due to carboxylic and hydroxyl species that were proposed the structure in previous literatures by Sammon, et al. [34, 43]. The proposed structures of hydroxyl species were shown in Fig. 4.14.

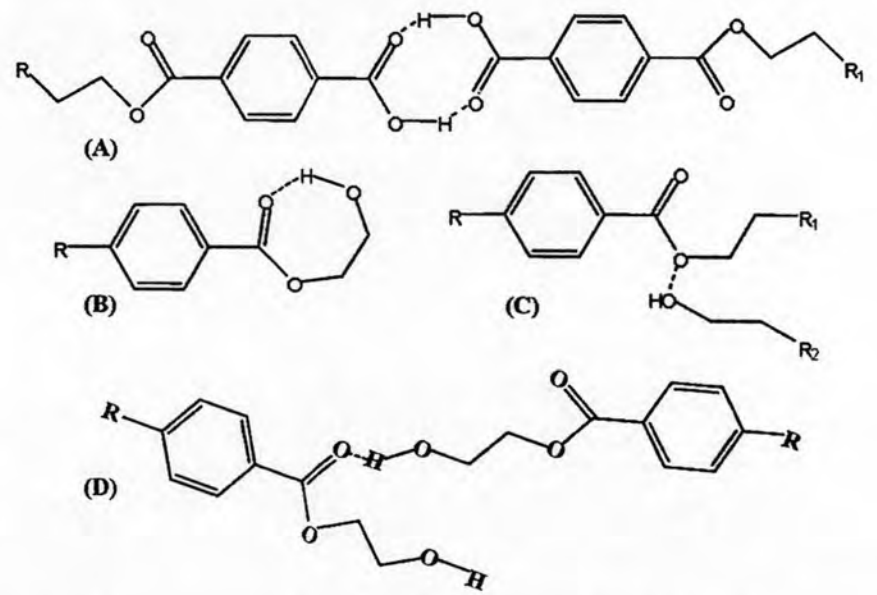


Fig. 4.14 The proposed hydrogen bonding of degraded PET structures.

As the curve fitting results, the hydroxyl compositions of irradiated PET by UV transmission showed the maxima at lower wavenumber. Whilst, the irradiated PET under the UV evanescent field had a maximum at the higher wavenumber. The hydroxyl band at lower wavenumber indicated the polymeric water in PET structure. The monomeric and dimeric water show absorption at higher wavenumber (as well as free hydroxyl peak). Therefore, the spectra of irradiated PET under the UV evanescent field irradiation revealed the free hydroxyl species more than that of irradiated PET by UV transmission. Furthermore, the curve fitting of carbonyl region

of irradiated PET under the UV evanescent field irradiation was different from that of UV transmission, as shown in Fig. 4.15.

The fitting of carbonyl band (1600-1800 $cm^{-1}$) of the un-irradiated PET showed one component of ester carbonyl at 1715 $cm^{-1}$. The bands of irradiated PET under the UV evanescent field irradiation and UV transmission consist of three and four carbonyl components, respectively. The carbonyl bands of the irradiated PET under the UV evanescent field irradiation consisted of ester group, carboxylic end group and aldehyde end group. The irradiated PET by UV transmission showed the anhydride component at 1781 $cm^{-1}$ and 1613 $cm^{-1}$[27].

The fitting results of carbonyl bands supported chemical changes during photo-degradation by both UV irradiations. There are the evidences for the existing of new hydrophilic species after the irradiation. The new irradiation generated species that have high polarity than the ester group of the un-irradiated PET.

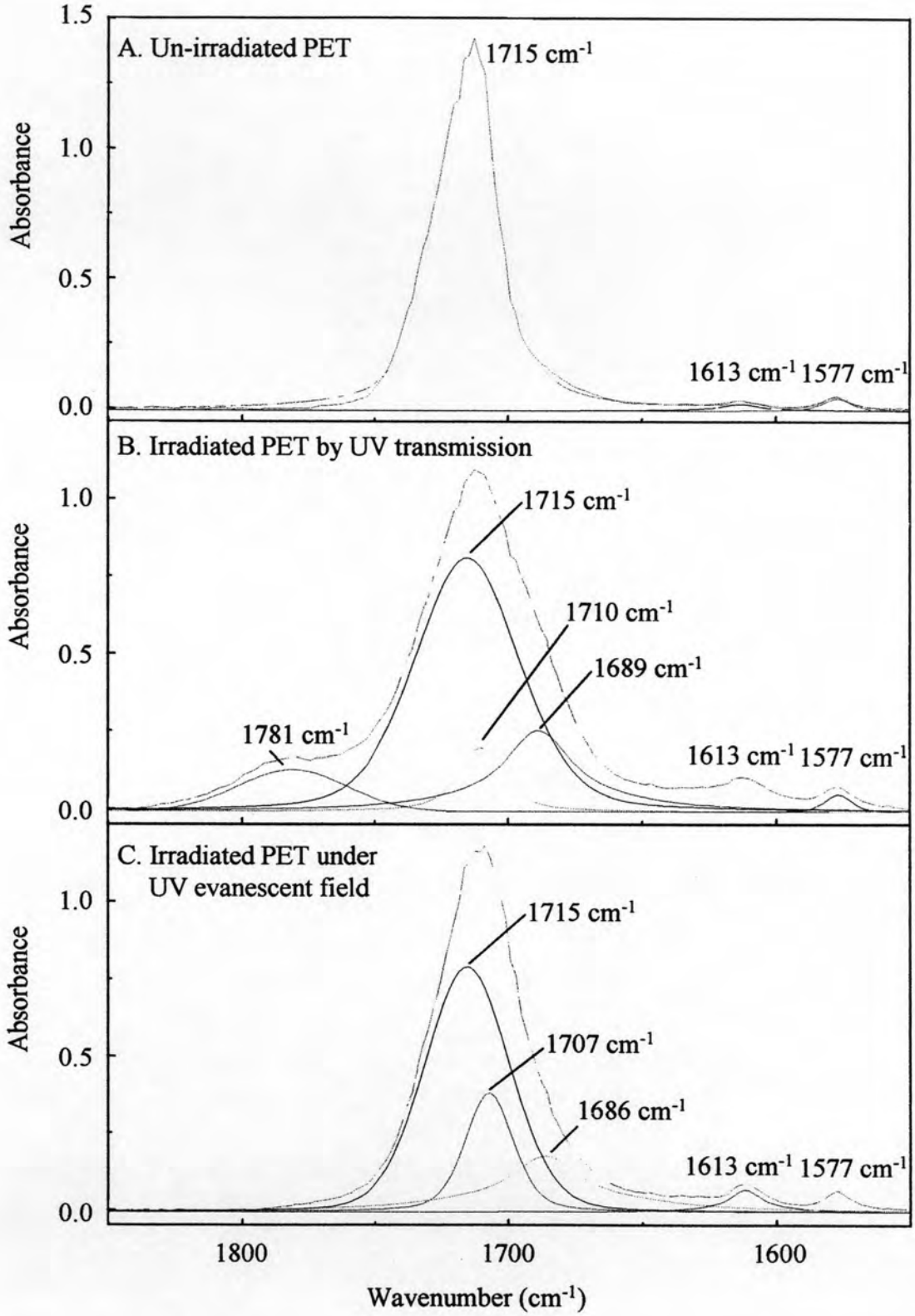


Fig. 4.15 Curve fitting of carbonyl band of un-irradiated PET and irradiated PET: (A) un-irradiated PET, (B) irradiated PET by transmission, and (C) irradiated PET by UV evanescent field irradiation.

### 4.3.2 FT-Raman spectroscopy

The Raman spectroscopy shows the molecular information of the molecule, which is changing the polarizability. Raman spectroscopy is the complementary technique to the infrared technique. When IR and Raman techniques are employed, the completely molecular informations are obtained. Therefore, the Raman results are supporting that of the IR results.

Raman spectrum of an un-irradiated PET was collected by FT-Raman spectrometer. Peak assignments of PET are shown in Table 4.5 [9, 44-45]. The FT-Raman spectrum of the un-irradiated PET was compared with that of irradiated PET (i.e., both irradiation techniques), Fig. 4.16.

The Raman spectrum of the irradiated PET by UV transmission was different from that of the un-irradiated PET and the irradiated PET under the UV evanescent field as the baseline shift and spectra changes were clearly observed. The Raman spectra of irradiated PET by UV transmission showed the following spectral features: splitting peak at 1095 $cm^{-1}$, increasing peak height at 999 $cm^{-1}$, decreasing peak height at 884 $cm^{-1}$ (*gauche* structure in ethylene glycol segment) and increasing of sharp peak intensity at 857 $cm^{-1}$. These spectral features were not observed in the Raman spectra of un-irradiated PET and irradiated PET under the UV evanescent field irradiation. The spectral intensity changes of the irradiated PET by the UV transmission indicated an increasing of the crystallinity as discussed previously in the ATR FT-IR spectroscopy section. This observed crystallinity change which obtained from Raman spectra supported the spectra changes observed in ATR FT-IR spectra. Moreover, the chromophore formations from photo-degradation which affect the baseline shift of Raman spectra also supported the observed color change of the irradiated PET sample by UV transmission. The degraded products of the irradiated PET by UV transmission which was composed of the chromophore groups cause the fluorescent emission when it was excited by laser source of the Raman spectrometer. The fluorescent radiation was emitted, that affects the Raman scattering detection. As a result, the Raman spectra of irradiated PET by UV transmission showed baseline shift due to color formation of chromophore groups. On the other hand, the Raman spectra acquisition of un-irradiated PET and irradiated PET under the UV evanescent

field were almost the same. This indicated an unchanged bulk property of PET under the UV evanescent field irradiation. Raman spectra of PET film at the surface and that at the greater depth were shown in Fig. 4.17.

From Fig. 4.17, the FT-Raman spectra of transparent PET film were collected from the surface and at greater depths that showed the same spectral information. The Raman scattering intensity was decreasing as the focal point became deeper (i.e., 400, 800, 1200 μm from the surface). Since these results can support the chemical information of the bulk, the Raman spectra of irradiated PET by both the exposed side and opposite side were collected and compared with that of un-irradiated PET (i.e., similar comparison performed in the ATR experiments).

The Raman spectra of both the exposed side and the opposite side of irradiated PET by UV transmission were compared with that of un-irradiated PET that shown in Fig. 4.18. The spectral features of the exposed side were similar with that of the opposite side. However, the baseline shift of exposed side was greater than the opposite side due to the intensive fluorescent emission (i.e., as discussed in section 4.21). When the Raman spectra of irradiated PET by UV transmission by both exposed side and opposite side were compared with that of un-irradiated PET, obvious differences were observed (i.e., a splitting peak at 1097 $cm^{-1}$, increasing peak at 999 $cm^{-1}$, decreasing peak at 884 $cm^{-1}$, and increasing in sharp peak at 857 $cm^{-1}$), as shown in Fig. 4.19.

The FT-Raman spectra of the exposed side and the opposite side of irradiated PET under the UV evanescent field irradiation were similar with that of un-irradiated PET as shown in Fig. 4.20.

The irradiated PET under the UV evanescent field irradiation showed the unchanged spectral features associated with the bulk properties. These Raman results were supporting evidences for assuring that change of irradiated PET under the UV evanescent field occurred at the surface only. However, the changes of irradiated PET by UV transmission occur in the greater depth.

Table 4.5 FT-Raman bands assignment of PET spectrum.

| Raman shift ($cm^{-1}$) | Bands assignment |
|---|---|
| 3080 | Aromatic C-H stretching |
| 2964, 2907 | Aliphatic C-H stretching |
| 1726 | C=O stretching |
| 1614 | C=C aromatic ring |
| 1459 | C-H deformation, residual glycol in PET film |
| 1414 | C-C stretching of aromatic ring |
| 1372 | $CH_2$ wagging |
| 1288 | Aromatic ring and O-C stretching |
| 1184 | C-H in plane bending of aromatic ring |
| 1116, 1095 | C-H in plane bending and C-O stretching |
| 999 | C-C stretching, glycol |
| 857 | C-C breathing |
| 795 | C-C out of plane of aromatic ring |
| 703 | C-C-C out of plane of aromatic ring |
| 632 | C-C-C in plane bending of aromatic ring |

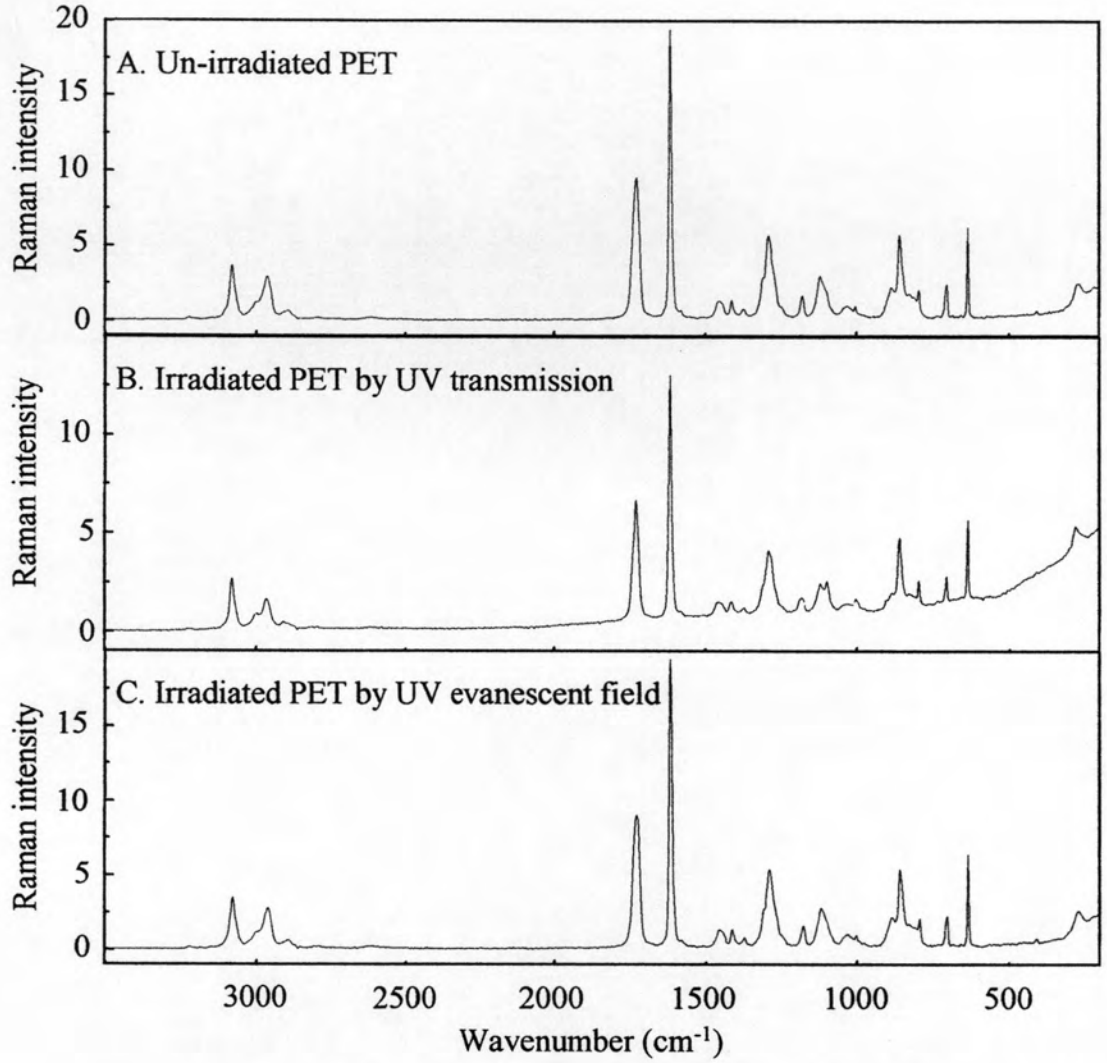


Fig. 4.16 FT-Raman spectra of un-irradiated PET with irradiated PET at 10 minutes irradiation time: (A) un-irradiated PET, (B) irradiated PET by UV transmission, and (C) irradiated PET under UV evanescent field.

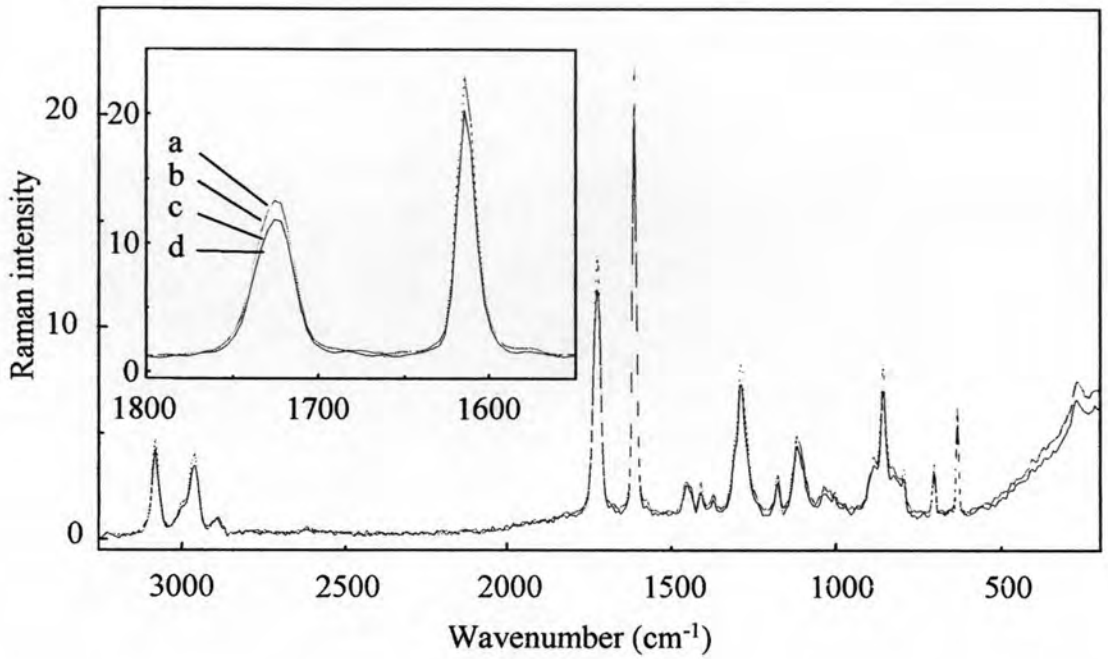


Fig. 4.17 FT-Raman spectra of transparent PET at various focusing point from the surface: (a) at the surface, (b) at 400 μm from the surface, (c) at 800 μm from the surface, and (d) at 1200 μm from the surface.

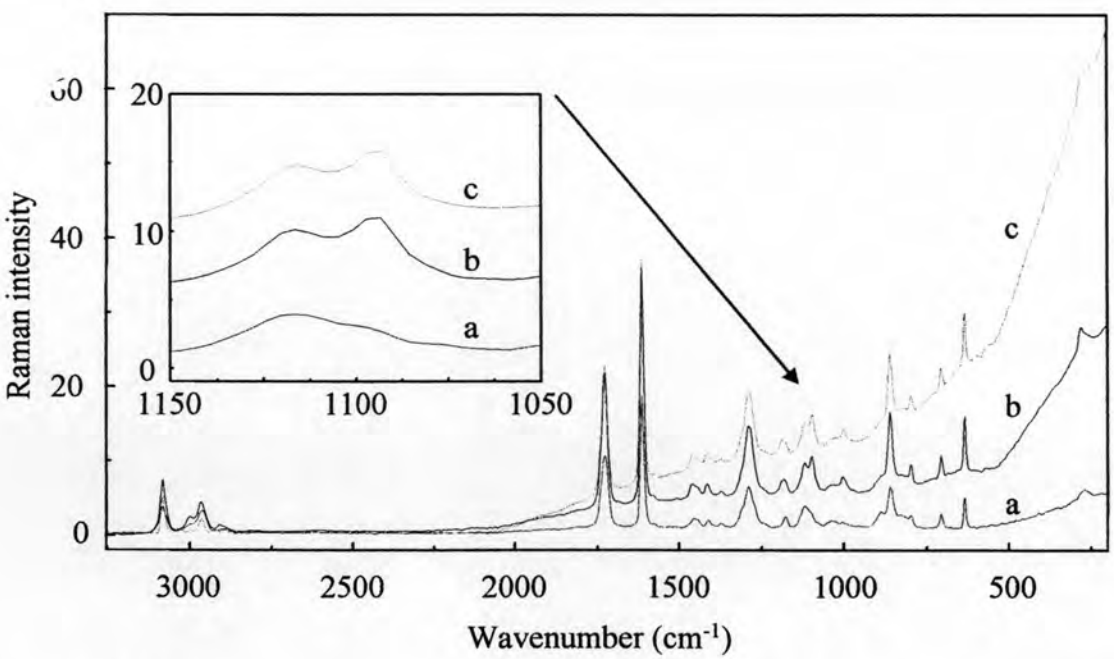


Fig. 4.18 FT-Raman spectra of the irradiated PET by UV transmission: (a) an un-irradiated PET, (b) the opposite side, and (c) the exposed side of the irradiated PET.

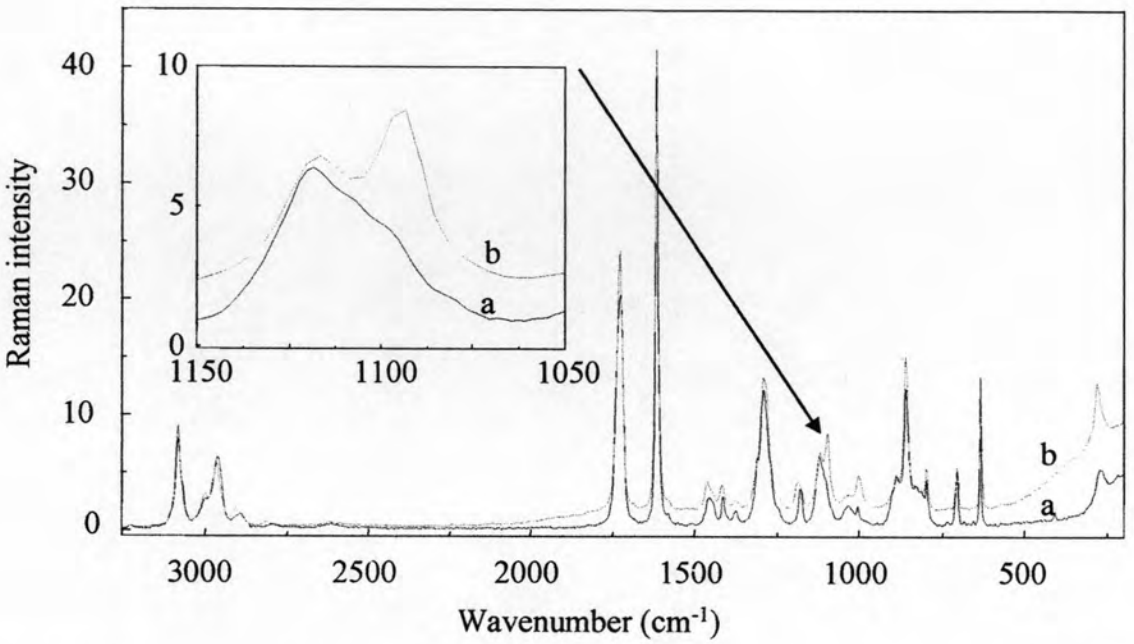


Fig. 4.19 The un-irradiated PET spectra compared with that of annealed PET: (a) un-irradiated PET and (b) annealed PET.

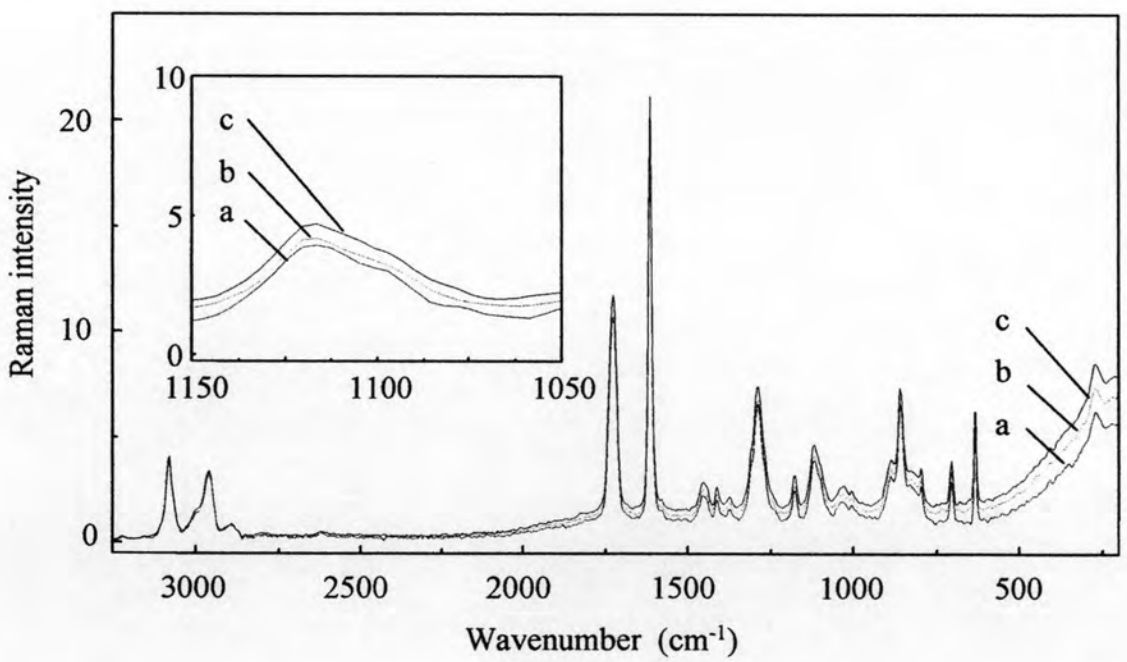


Fig. 4.20 FT-Raman spectra of irradiated PET under the UV evanescent field irradiation: (A) un-irradiated PET (B) opposite side and (C) exposed side.

### 4.3.3 Photo-degradation mechanisms

According to literatures [6, 35], the photo-degradation mechanisms of PET have been proposed that the degraded products occurred in various pathways due to several reactions such as photo-oxidation, photolysis, and photo-hydrolysis. These processes needed the appropriate condition. The observed ATR FT-IR and Raman spectra of irradiated PET by both irradiations were concluded and proposed the possible pathways that occurred with the irradiated PET samples of this research. These possible pathways were shown in Fig. 4.21

The photo-degradation processes of PET can create the carboxylic, aldehyde, anhydride and colored species. According to the ATR FT-IR and FT-Raman results, the carboxylic and aldehyde groups were found in irradiated PET by both irradiation techniques. The anhydride and colored species were observed only in the irradiated PET by UV transmission. From Fig. 4.21, the carboxylic group was produced in pathway A and B that followed to Norrish type II and photolysis, respectively. The aldehyde and anhydride groups were showed in the photolysis reaction (pathway C) and photo-oxidation reaction (pathway E), respectively. The colored species that can be obviously seen from the external PET texture of irradiated PET by UV transmission followed pathway D, which showed the dihydroxyl and quinone compounds associated with the fluorescence in the observed Raman spectra of irradiated PET by UV transmission.

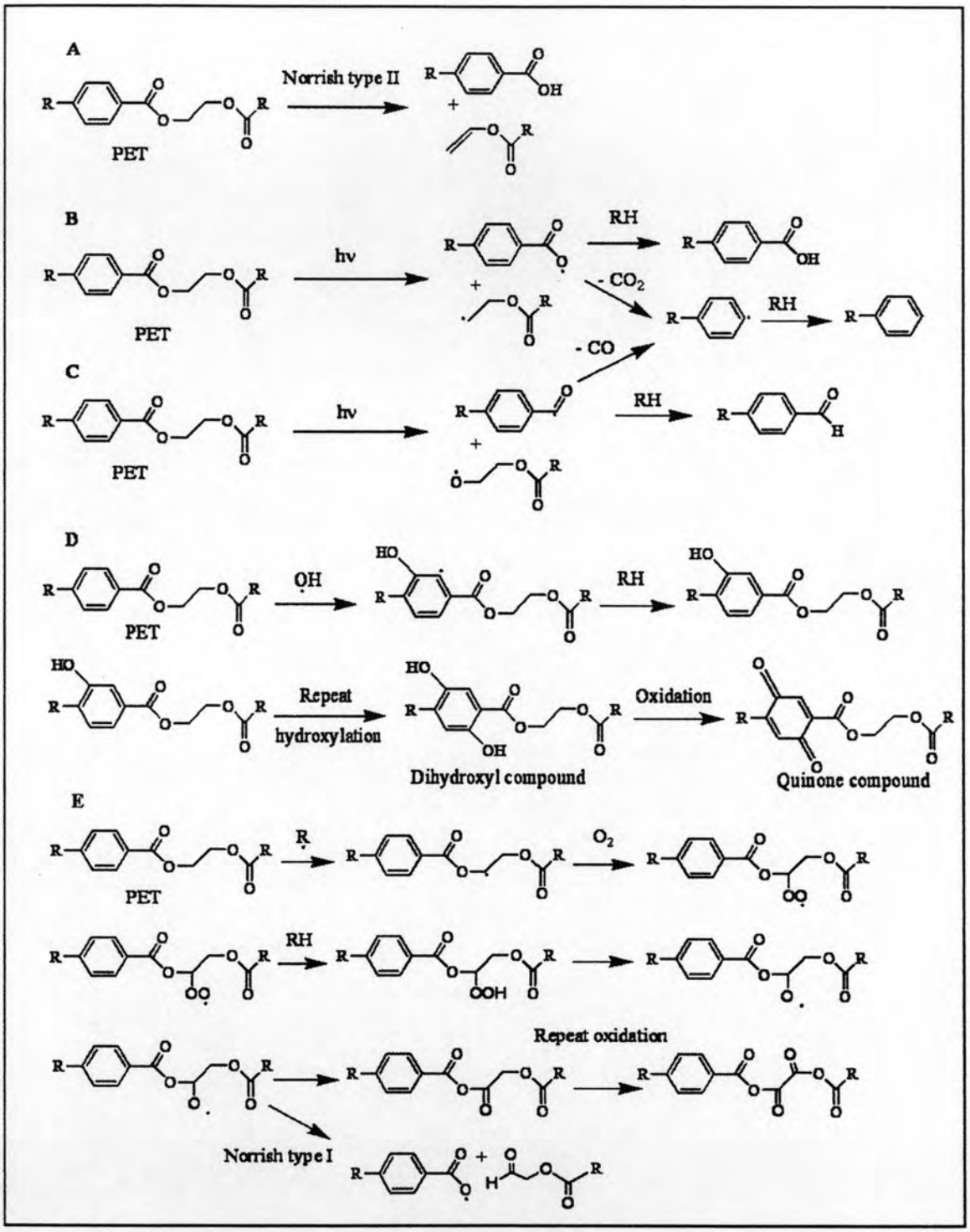


Fig. 4.21 The photo-degradation pathways of irradiated PET by UV transmission and the UV evanescent field irradiation.

## 4.4 UV evanescent field induced surface degradation of various PET

The PET film samples were studied in previous section. Nevertheless, PET was made into various forms. The PET fiber was a widely employed form in textile industries. This research was also interested in various form of PET that may be affected by the photo-degradation process. In this section, the various PET forms were irradiated by the UV evanescent field irradiation.

The micro-fibers need the sample preparation on the specific holder before the spectra were collected due to inadequately contact between fibers and IRE. The PET fibers were twined in holder and supported by the polymer substrate that can be improved ATR contact. However, the substrate affects the ATR spectra acquisition, if the diamond IRE penetrates into the substrate. Therefore, ATR spectrum of the substrate was collected before that of the fibers. The infrared spectrum of the substrate was compared with the PET spectrum in order to make sure that the purely PET spectra were obtained. The infrared spectrum of polycarbonate (PC) substrate was shown in Fig. 4.22.

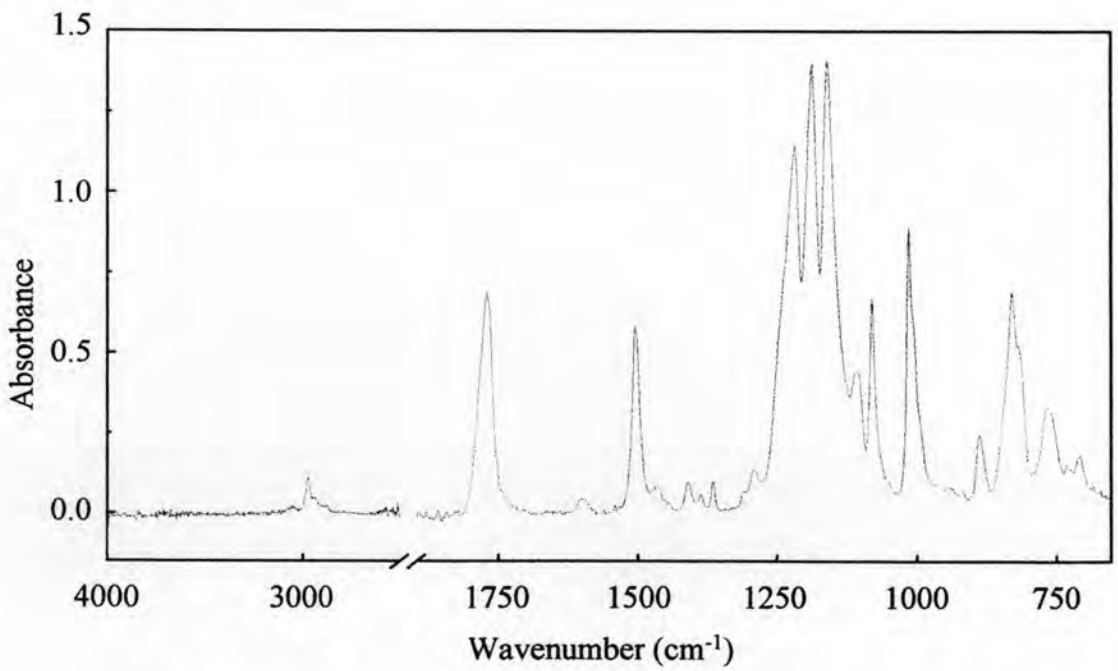


Fig. 4.22 ATR FT-IR spectrum of polycarbonate (PC) substrate.

### 4.4.1 Staple fiber

The staple fiber is a synthetic fiber, which has the length less then 18 inches. The staple fibers were exposed for 1-10 minutes under the UV evanescent field irradiation. ATR spectra of the irradiated and the un-irradiated staple fiber were shown in Fig. 4.23.

These observed spectra changes of irradiated PET staple fibers under the UV evanescent field at various irradiation times showed that the absorption at 1338 $cm^{-1}$ was almost unchanged. This implied the conformation changes of irradiated PET staple fiber were less than that of the irradiated PET film. This may be due to the high crystalline content in the PET staple fiber (which is greater than that of the PET film). From these results, the irradiated PET staple fiber under the UV evanescent field showed the existing of hydrophilic species at the surface, but the magnitude was less than that of the irradiated PET film.

### 4.4.2 Filament yarns

The PET filament yarns (i.e., spin draw yarn (SDY) and draw textured yarn (DTY)) were irradiated by the UV evanescent field for 1-10 minutes. ATR FT-IR spectra of the irradiated yarn and the un-irradiated yarn were shown in Fig. 4.24 and Fig. 4.25.

Both SDY and DTY spectra showed the hydroxyl band, band broadening of carbonyl and crystalline phase transformation to amorphous phase. The magnitude of the changes increased as the irradiation time increased. These changes were similar to those of the irradiated PET staple fiber and the irradiated PET film under the UV evanescent field irradiation. This supported the degradation of PET, which can be improved the hydrophilicity at the surface. Moreover, the observed infrared spectra of irradiated PET both SDY and DTY under the UV evanescent field irradiation were a good supporting evidence for improving hydrophilicity of high crystallinity PET.

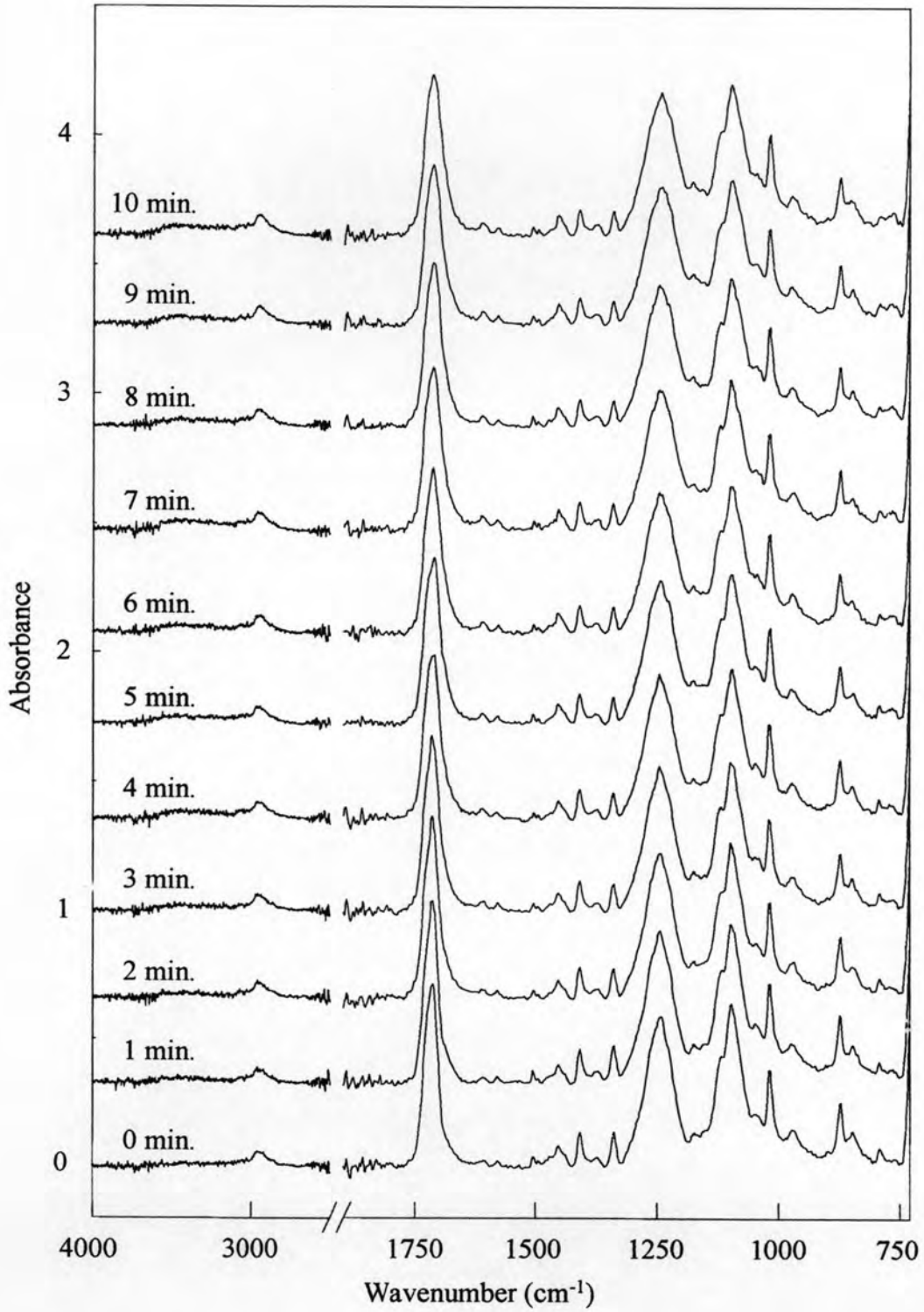


Fig. 4.23 ATR FT-IR spectra of irradiated staple fiber under the UV evanescent field irradiation for 1-10 minutes irradiation time and that of un-irradiated PET (0 minute).

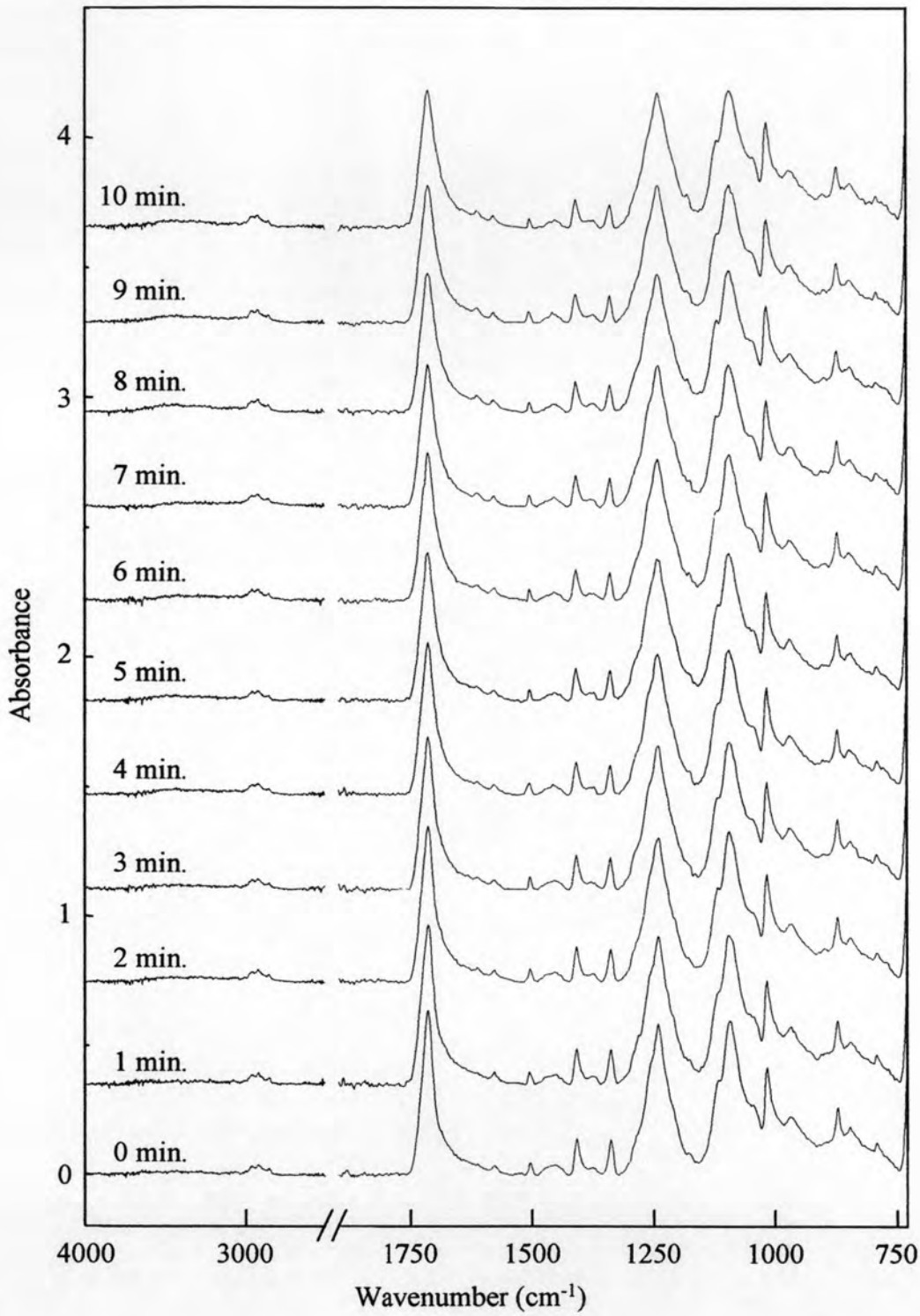


Fig. 4.24 ATR FT-IR spectra of irradiated SDY PET filament under the UV evanescent field irradiation for 1-10 minutes irradiation time and that of un-irradiated PET (0 minute).

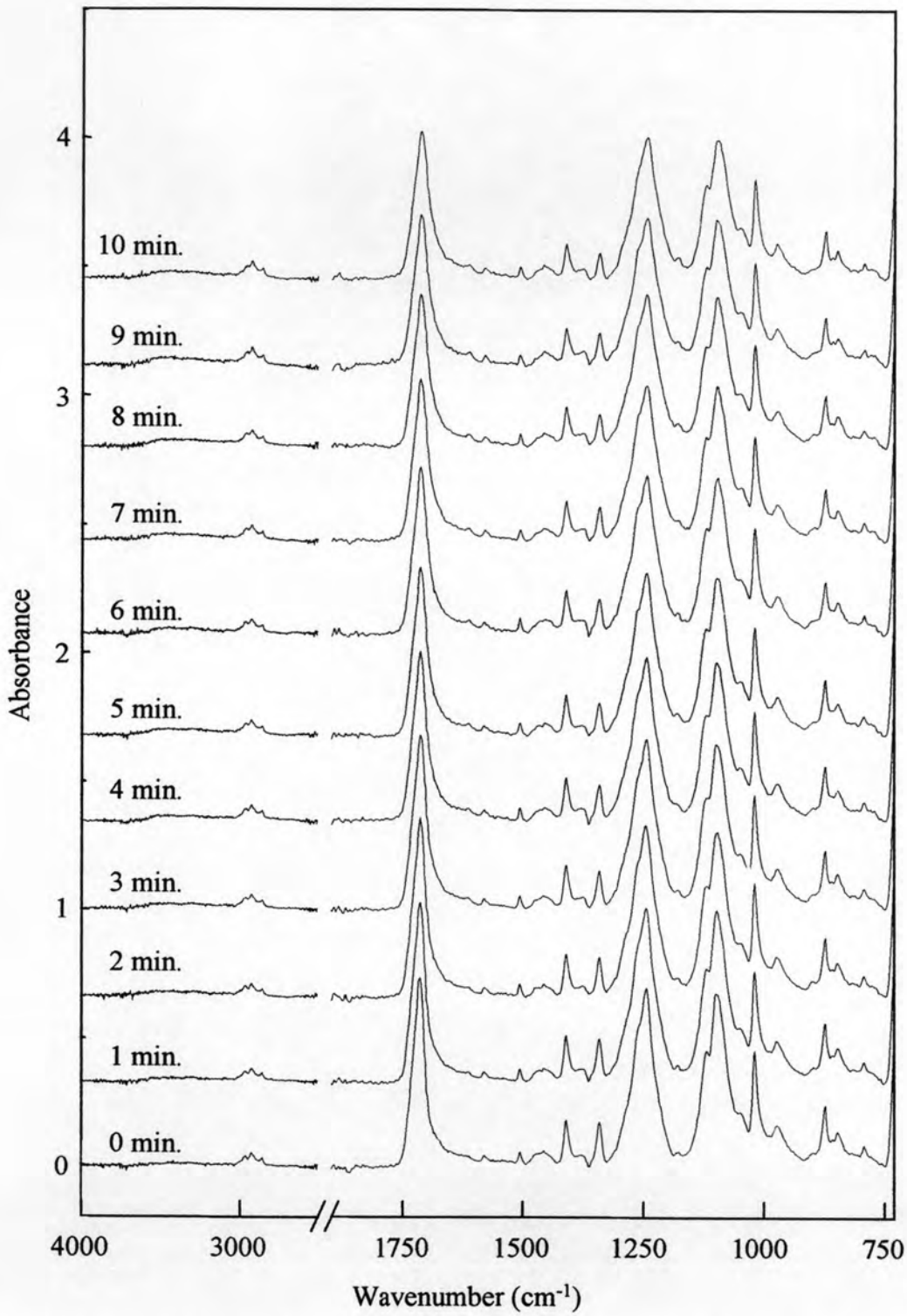


Fig. 4.25 ATR FT-IR spectra of irradiated DTY PET filament under the UV evanescent field irradiation for 1-10 minutes irradiation time and that of un-irradiated PET (0 minute).

## 4.5 Stability of hydrophilic species of irradiated PET under the UV evanescent field

At the ambient condition, ageing can affect the hydrophilic species of the irradiated PET surface due to moisture, temperature, and radiation. Therefore, the hydrophilic species which were induced by UV evanescent field irradiation were studied the stability under the ambient condition. The irradiated PET films under the UV evanescent field for 1-10 minutes were kept for three months at ambient condition and repeatedly collected the ATR FT-IR. The results were shown in Fig. 4.26.

The ATR FT-IR spectral features of the irradiated PET film at various irradiation times showed no sign of change after three months storage. This indicated the high stability of hydrophilic species at the surface. When the irradiated PET was subsequently analyzed after the storage, the sampling position on the PET surface was slightly changed. This can influence the observed spectral quality for quantitative analysis. However, it did not affect the qualitative analysis. Thus, the observed spectra indicated the stability of the hydrophilic species at the PET surface. These results were important for many industries since good stability of hydrophilic species implied a long shelf life or service time of the products.

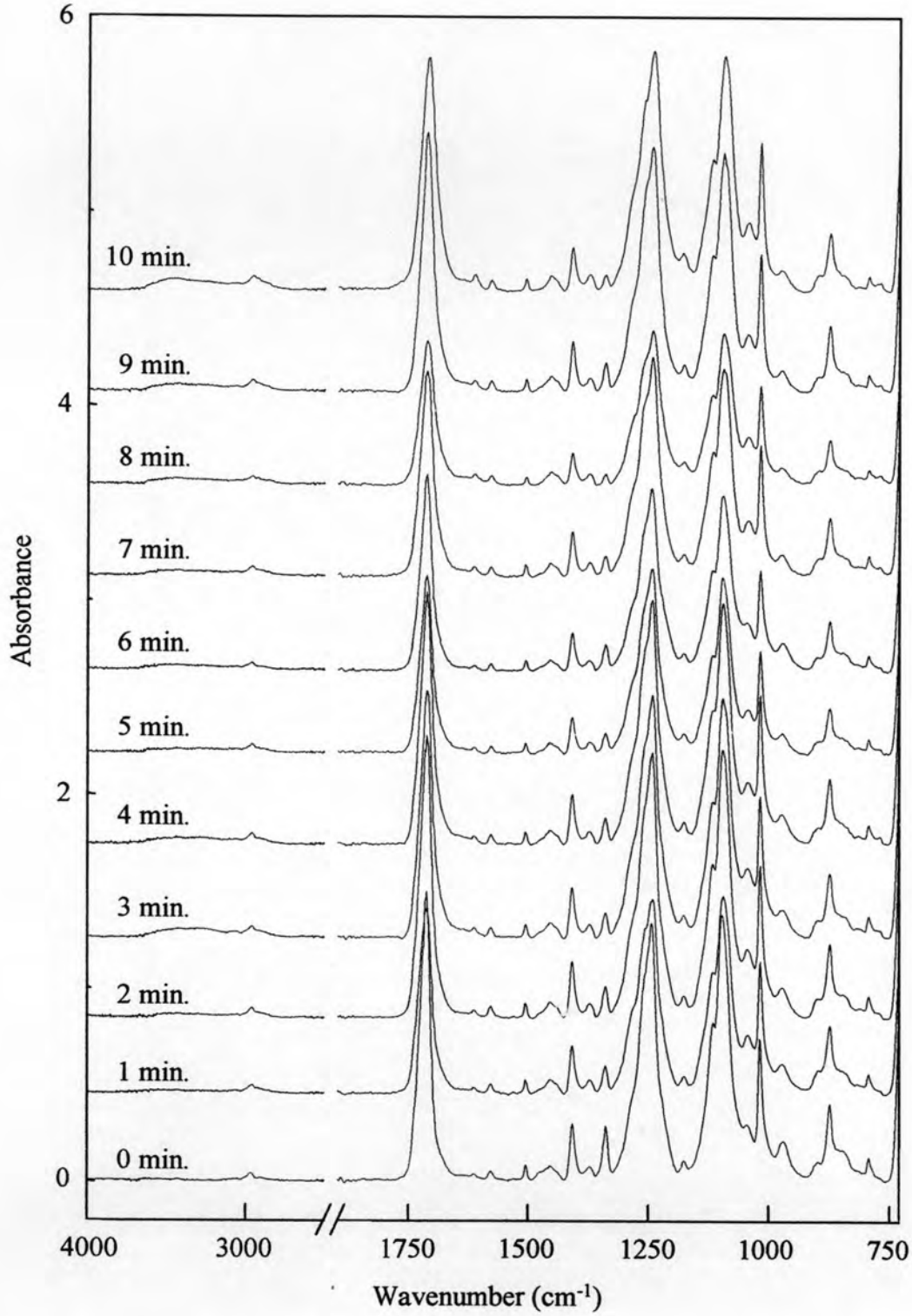


Fig. 4.26 ATR FT-IR spectra of PET film irradiated for 1-10 minutes and the un-irradiated PET after a three-month storage at the ambient condition.